

Phosphorylation of STIM1 at ERK1/2 target sites regulates interaction with the microtubule plus-end binding protein EB1

Eulalia Pozo-Guisado¹, Vanessa Casas-Rua¹, Patricia Tomas-Martin¹, Aida M. Lopez-Guerrero¹, Alberto Alvarez-Barrientos² and Francisco Javier Martin-Romero^{1,*}

¹Department of Biochemistry and Molecular Biology, College of Life Sciences, University of Extremadura, Badajoz 06006, Spain

²Bioscience Applied Techniques Facility, University of Extremadura, Badajoz 06006, Spain

*Author for correspondence (fjmartin@unex.es)

Accepted 26 April 2013

Journal of Cell Science 126, 3170–3180

© 2013. Published by The Company of Biologists Ltd

doi: 10.1242/jcs.125054

Summary

STIM1 (stromal interaction molecule 1) is a key regulator of store-operated calcium entry (SOCE). Upon depletion of Ca²⁺ concentration within the endoplasmic reticulum (ER), STIM1 relocalizes at ER-plasma membrane junctions, activating store-operated calcium channels (SOCs). Although the molecular details for STIM1-SOC binding is known, the regulation of SOCE remains largely unknown. A detailed list of phosphorylated residues within the STIM1 sequence has been reported. However, the molecular pathways controlling this phosphorylation and its function are still under study. Using phosphospecific antibodies, we demonstrate that ERK1/2 mediates STIM1 phosphorylation at Ser575, Ser608 and Ser621 during Ca²⁺ store depletion, and that Ca²⁺ entry and store refilling restore phosphorylation to basal levels. This phosphorylation occurs in parallel to the dissociation from end-binding protein 1 (EB1), a regulator of growing microtubule ends. Although Ser to Ala mutation of residues 575, 608 and 621 showed a constitutive binding to EB1 even after Ca²⁺ store depletion, Ser to Glu mutation of these residues (to mimic the phosphorylation profile attained after store depletion) triggered full dissociation from EB1. Given that wild-type STIM1 and STIM1^{S575E/S608E/S621E} activate SOCE similarly, a model is proposed to explain how ERK1/2-mediated phosphorylation of STIM1 regulates SOCE. This regulation is based on the phosphorylation of STIM1 to trigger dissociation from EB1 during Ca²⁺ store depletion, an event that is fully reversed by Ca²⁺ entry and store refilling.

Key words: STIM1, Calcium, Store-operated calcium entry, EB1, Phosphorylation, ERK1/2

Introduction

STIM1 (stromal interaction molecule 1), a single-transmembrane protein that acts as a Ca²⁺ sensor within the luminal space of the endoplasmic reticulum (ER), is a key regulator of store-operated calcium entry (SOCE) (Liou et al., 2005; Roos et al., 2005; Zhang et al., 2005). STIM1 oligomerizes upon depletion of Ca²⁺ concentration within the ER, and relocalizes in puncta-like ER-plasma membrane (PM) junctions (Liou et al., 2007; Muik et al., 2008; Smyth et al., 2008). This oligomerization and relocalization of STIM1 is required for the activation of SOCE by means of the binding to store-operated calcium channels (SOCs), including ORAI1 (Feske et al., 2006; Soboloff et al., 2006; Vig et al., 2006; Yeromin et al., 2006; Zhang et al., 2006) and some of the transient receptor potential canonical (TRPC) channels (Yuan et al., 2007). However, TRPC channels can function in STIM1-dependent and STIM1-independent modes, and the ratio of STIM1/TRPC determines the STIM1-dependent mode of the channels to tune their SOC-dependent and SOC-independent functions (Lee et al., 2010). Activation of ORAI1 requires the interaction of coiled-coil domains with the cytosolic domain of STIM1 named STIM1-ORAI1 activation region (SOAR) or CRAC activation domain (CAD) (Muik et al., 2008; Park et al., 2009; Yuan et al., 2009). This SOAR/CAD encompasses residues 334–442 of STIM1 organized in two coiled-coil (CC) domains (CC2 and CC3). The interaction of

CC1 with CC2/CC3 keeps STIM1 in a closed conformation in the resting state, and the binding of STIM1 with ORAI1 requires an intramolecular transition of STIM1 into an open conformation, thereby exposing CC2 and CC3 (Korzeniowski et al., 2010; Muik et al., 2011). It has been shown that STIM1 also binds to voltage-operated Ca²⁺ (Ca_v1.2) channels, although in this case it suppresses activation of these channels while activating ORAI channels, with both actions being mediated by the SOAR/CAD domain of STIM1 (Park et al., 2010; Wang et al., 2010). STIM1 has a serine/proline-rich domain, with unknown function, and a polybasic, lysine-rich domain which is involved in the clustering of STIM1 at the PM (Liou et al., 2007), and the gating of TRPC channels (Lee et al., 2010; Zeng et al., 2008).

Although most of the studies on the molecular mechanism of the activation of SOCs have focused on the minimal domain of cytosolic STIM1 required for this activation, many aspects of this mechanism remain unknown. In seeking the molecular mechanisms that make STIM1 able to discriminate between channels (ORAI channels versus TRPCs), and sometimes to trigger opposing actions (as in SOCs versus Ca_v1.2 channels), one finds that the cytosolic side of STIM1 presents another important domain, the Ser/Pro (or S/P)-rich domain, which could be acting as a key modulator of these channels. STIM1 is a phosphoprotein (Manji et al., 2000), and a detailed list of phospho-residues has

been reported (Pozo-Guisado et al., 2010; Smyth et al., 2009; Yu et al., 2009). However, neither the molecular pathway that controls STIM1 phosphorylation nor the biological function of many of the phosphorylated residues are known. A report from our laboratory has shown that extracellular signal-regulated kinases 1/2 (ERK1/2) phosphorylate STIM1 *in vitro* at Ser575, Ser608 and Ser621, and that the increase of phosphorylation at PXPSP or pSPXR/K motifs *in vivo*, revealed by an anti-phospho-MAPK/CDK substrate antibody, suggests an increase in STIM1 phosphorylation at ERK1/2 target sites during SOCE activation. Additionally, Ser to Ala mutation of target residues strongly reduces Ca^{2+} entry and decreases STIM1-ORAI1 binding, as monitored by fluorescence resonance energy transfer (FRET) or by co-immunoprecipitation (Pozo-Guisado et al., 2010), supporting the requirement of STIM1 phosphorylation at Ser575, Ser608 and Ser621 to achieve full activation of SOCE in asynchronous cultures of HEK293 cells. In addition to HEK293 cells, STIM1 phosphorylation, detected by an anti-phospho-MAPK/CDK substrate antibody, is enhanced by thapsigargin in neonatal rat ventricular myocytes (Zhu-Mauldin et al., 2012). Moreover, it has been reported that STIM1 phosphorylation at Ser575 promotes C2C12 myoblasts differentiation to myocytes (Lee et al., 2012), and that Ser to Ala mutation of residues 575, 608, and 621 impairs platelet adhesion to fibrinogen (Evers et al., 2012), further supporting a role for STIM1 phosphorylation in cell physiology.

A point of intense debate is the regulation of SOCE by the microtubule cytoskeleton. It was early suggested that STIM1 localization and function involves the microtubule cytoskeleton because inhibition of microtubule depolymerization severely affected SOCE (Smyth et al., 2007). Other studies, however, did not observe any effect of nocodazole on SOCE in RBL-1 cells and NIH 3T3 cells (Bakowski et al., 2001; Ribeiro et al., 1997). STIM1 directly binds to EB1 (end-binding protein 1), a well known regulator of growing microtubule ends (Grigoriev et al., 2008). Therefore, STIM1 has been described as a microtubule plus-end-tracking protein (+TIP), and its subcellular localization is dependent on microtubule formation (Grigoriev et al., 2008; Smyth et al., 2007). But it is unclear whether microtubules modulate the rearrangement of both STIM1 and ORAI1 into puncta-like structures as a result of Ca^{2+} store depletion. It was later demonstrated that a STIM1 sequence encompassing residues 642–645 (residues Thr-Arg-Ile-Pro, or TRIP) is critical for the binding to EB1 (Honnappa et al., 2009). A similar sequence (S/TxIP) is found in other +TIPs (Tamura and Draviam, 2012), and for some of these EB1 interactors, such as CLASP2 and APC, it was found that the phosphorylation of the +TIP regulates the association to EB1 (Kumar et al., 2009; Watanabe et al., 2009; Zumbunn et al., 2001).

In the present work, we demonstrate that ERK1/2 mediates STIM1 phosphorylation at Ser575, Ser608 and Ser621 during Ca^{2+} store depletion, and that Ca^{2+} entry and store refilling restore phosphorylation to basal levels. Also, we demonstrate that phosphorylation of STIM1 at Ser575, Ser608 and Ser621 regulates the interaction with EB1. Finally, we propose a model to explain the regulation of SOCE and the binding to EB1 based on the phosphorylation of STIM1.

Results

Phosphorylation of STIM1 at Ser575, Ser608 and Ser621 under store depletion conditions

We have developed phosphospecific antibodies against Ser575, Ser608 and Ser621, to demonstrate STIM1 phosphorylation *in*

in vivo during SOCE activation. For that purpose we used HEK293 Fln-In T-REx cells stably transfected for the inducible expression of tagged STIM1. We show here that Ca^{2+} store depletion, triggered with thapsigargin (Tg), led to a significant increase of STIM1 phosphorylation at Ser575, Ser608 and Ser621 in HEK293 cells overexpressing FLAG-STIM1 (Fig. 1A). Overexpression of STIM1 with alanine substitution mutations at these sites, i.e. FLAG-STIM1^{S575A/S608A/S621A}, completely suppressed the phosphorylation signal, confirming the specificity of the antibodies against phospho-residues. Moreover, phosphorylation of Ser575, Ser608 and Ser621 was fully prevented by PD0325901 or PD184352 (Fig. 1B), two potent and selective inhibitors of the activation of ERK1/2 by MEK1/2 (Bain et al., 2007), and recognized inhibitors of SOCE in HEK293 cells (Pozo-Guisado et al., 2010). In addition to the previously reported role of ERK1/2 in the phosphorylation of STIM1 *in vitro* (Pozo-Guisado et al., 2010), the results shown here demonstrate that ERK1/2 phosphorylates STIM1 at Ser575, Ser608 and Ser621 *in vivo*. We studied the kinetics of STIM1 phosphorylation at residues 575, 608, and 621 by monitoring the time-course of STIM1 phosphorylation in HEK293 cells under store depletion conditions, triggered by Tg. We observed that this phosphorylation increased significantly after 5 minutes for the three sites (Fig. 2). This kinetics of STIM1 phosphorylation correlates with the kinetics of ERK1/2 activation that we observed during store depletion triggered by Tg, i.e. ERK1/2 was activated shortly before STIM1 phosphorylation, an additional result that supports a relationship between the two events, in agreement with our previously reported *in vitro* studies (Pozo-Guisado et al., 2010).

To study whether STIM1 phosphorylation is reversed by the cessation of SOCE, we treated STIM1-GFP-expressing HEK293 cells with 10 μM TBHQ [2,5-di-(*tert*-butyl)-1,4-benzohydroquinone], a reversible inhibitor of the sarco(endo)plasmic reticulum Ca^{2+} -ATPase (SERCA) (Kass et al., 1989), in Ca^{2+} -free medium for 10 minutes. TBHQ was then removed by washing with Ca^{2+} -containing medium for an additional 5–15 minutes in order to facilitate the refilling of intracellular stores. We monitored total lysates with anti-phosphospecific antibodies, observing that Ca^{2+} store refilling and Ser575, Ser608 and Ser621 dephosphorylation were concomitant (Fig. 3A). A simple explanation of this result would be the inhibition of ERK1/2 activity by specific phosphatases during Ca^{2+} store refilling. We tested this hypothesis by monitoring phospho-ERK1/2 under the same experimental conditions, and observed that ERK1/2 becomes rapidly dephosphorylated upon Ca^{2+} entry and store refilling (the two bottom blots in Fig. 3A). Although the molecular identification of the phosphatases involved in this process is beyond the scope of this work, we demonstrate here the correlation between dephosphorylation of ERK1/2, i.e. inactivation of this kinase, and dephosphorylation of STIM1 in Ca^{2+} store refilling conditions.

STIM1 oligomerizes and relocalizes in puncta-like ER-plasma membrane (PM) junctions upon depletion of intraluminal Ca^{2+} concentration (Liou et al., 2007; Muik et al., 2008). For this reason, we monitored the clustering of STIM1-GFP in HEK293 cells under the treatment with TBHQ in order to validate the experimental procedure used here. Fig. 3B and supplementary material Movie 1 show proper reversion of STIM1-GFP clustering after TBHQ removal, indicating an efficient refilling

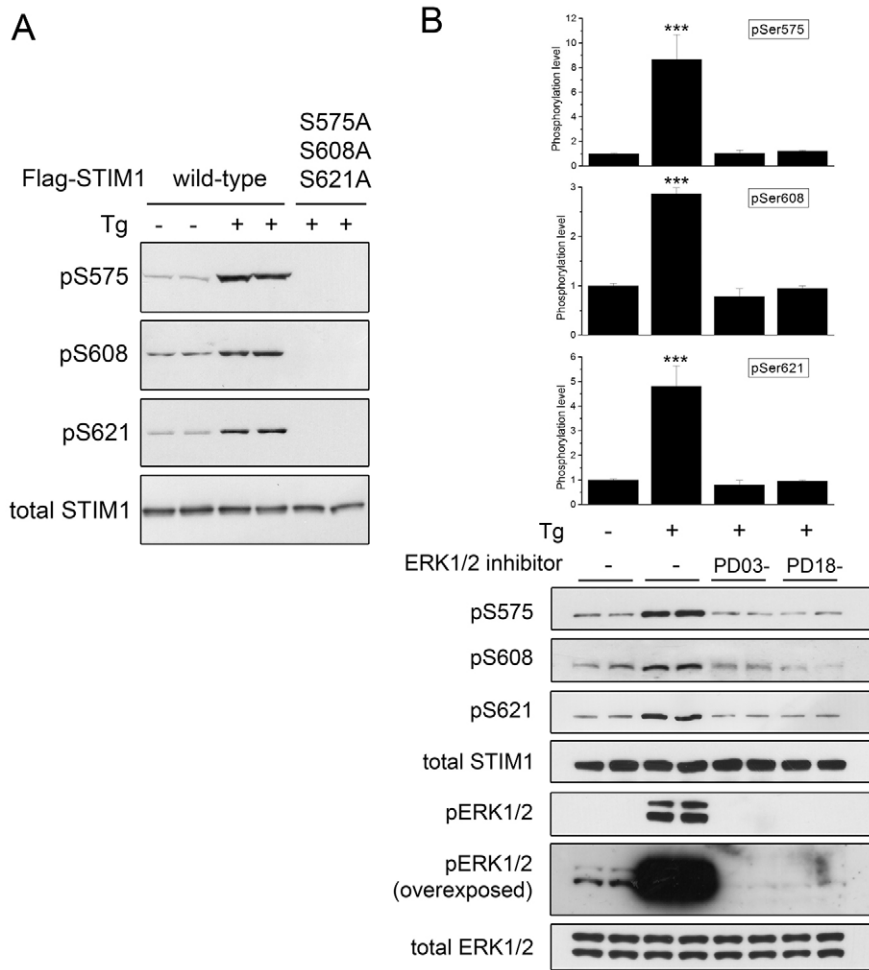


Fig. 1. *In vivo* phosphorylation of STIM1 at Ser575, Ser608 and Ser621. (A) HEK293 Flp-In T-REx cells were stably transfected for the inducible expression of FLAG-STIM1 (wild type) or FLAG-STIM1^{S575A/S608A/S621A}. Expression of tagged STIM1 was induced by addition of doxycycline 24 hours prior to the experiment. After 8 hours in serum-free medium, cells were incubated in Ca²⁺-containing HBSS (-Tg), or in Ca²⁺-free HBSS with 1 μ M thapsigargin for 10 minutes (+Tg). Total lysates were used to detect phospho-residues by immunoblot with phosphospecific anti-STIM1 antibodies (labeled as pS575, pS608, and pS621). In parallel, the total amount of STIM1 was evaluated using a commercial anti-STIM1 antibody (lower blot). (B) As for A, cells were incubated in Ca²⁺-containing HBSS (-Tg), or in Ca²⁺-free HBSS (+Tg) for 10 minutes. To inhibit ERK1/2, cells were pre-incubated for 10 minutes with 0.1 μ M PD0325901 or 2 μ M PD184352 prior to the treatment with Tg. ERK1/2 activation was monitored with an anti-phospho (pThr202/pTyr204) ERK1/2 antibody (labeled as pERK1/2). Loading control was monitored with a total anti-ERK1/2 antibody (lower blot). An overexposed anti-phospho-ERK1/2 blot is shown to visualize basal ERK1/2. Quantification of the phosphorylation level was performed by blot densitometry after subtracting the background for each blot lane, using the Quantity-One software. Blots are representative of three independent experiments with three different lysates; data correspond to the calculated mean \pm s.d. *** P <0.001 compared with the control (-Tg, -ERK inhibitors).

of Ca²⁺ stores in HEK293 cells. Our results therefore demonstrate that ERK1/2-mediated phosphorylation of STIM1 at Ser575, Ser608 and Ser621 is reversible and dependent on the filling state of intracellular Ca²⁺ stores.

Functional consequences of constitutive phosphorylation of STIM1

Because we observed a direct link between the level of Ca²⁺ within intracellular stores and STIM1 phosphorylation, we analysed the role of the phosphorylation at these sites in the activation of SOCE. We reported previously that SOCE is inhibited in cells expressing FLAG-STIM1 with Ser to Ala (S/A) mutations in those sites (Pozo-Guisado et al., 2010). Here we show that Ser to Glu (S/E) mutations, intended to mimic constitutive phosphorylation of STIM1, did not inhibit SOCE in HEK293 cells. On the contrary, we observed an increase of SOCE in FLAG-STIM1^{S575E/S608E/S621E} cells over FLAG-STIM1(wt) cells, although this increase was moderate (Fig. 4A). The fact that constitutively phosphorylated STIM1 at ERK1/2 target sites does not stimulate greater SOCE over wild-type STIM1 can be interpreted in combination with the results shown in Fig. 1. Because wild-type STIM1 becomes phosphorylated during store depletion induced by Tg, the behavior of wild-type STIM1 and STIM1^{S575E/S608E/S621E} is similar. To study further the physiological consequences of constitutive phosphorylation, we challenged cells with short pulses of ATP plus carbachol

(ATP+CCh) in Ca²⁺-free medium as a rapid stimulus that leads to store depletion (Pozo-Guisado et al., 2010), followed by the rapid addition of extracellular Ca²⁺ in order to refill intracellular Ca²⁺ stores. Wild-type STIM1-expressing cells were able to respond to every purinergic stimulation by releasing Ca²⁺ from intracellular stores. However, absence of extracellular Ca²⁺ (see Fig. 4B; grey line) led to a diminished Ca²⁺ release in subsequent pulses of ATP+CCh. This experiment confirms that expression of FLAG-STIM1(wt) supports rapid responses to stimuli that activate the phosphoinositide pathway. However, expression of FLAG-STIM1^{S575A/S608A/S621A} did not sustain the series of sequential Ca²⁺ releases in response to purinergic stimulation (Fig. 4C), which can be explained by the defective activation of SOC channels due to constitutive dephosphorylation of STIM1. Indeed, this result further supports previous observations that suggested a significant decrease in SOCE, triggered by Tg, in cells expressing FLAG-STIM1^{S575A/S608A/S621A} (Pozo-Guisado et al., 2010). However, the sequential Ca²⁺ release in FLAG-STIM1^{S575E/S608E/S621E} was similar to that observed in wild-type STIM1-expressing cells (Fig. 4C), indicating that there are no major functional differences between wild-type and constitutively phosphorylated STIM1 upon purinergic stimulation.

STIM1 phosphorylation and binding to EB1

The phosphorylation sites described above are located in the Ser/Pro-rich domain of STIM1, a domain with an unknown function.

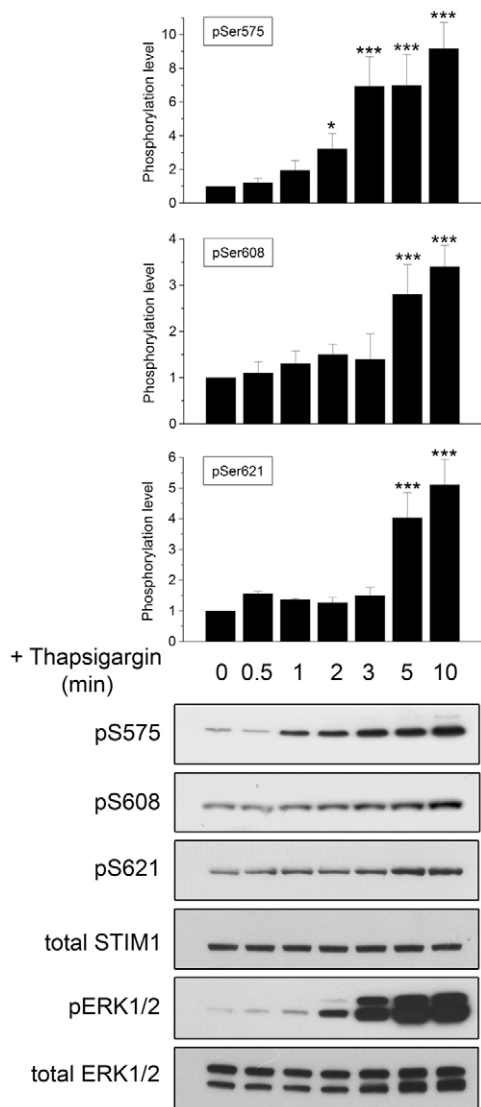


Fig. 2. Time-course of STIM1 phosphorylation under store depletion conditions. HEK293 Flp-In T-REx cells were stably transfected for the inducible expression of FLAG-STIM1. Other experimental conditions were as described for Fig. 1. Cells were incubated in Ca^{2+} -free HBSS with 1 μM thapsigargin for 0–10 minutes and the total lysates used to detect phospho-residues by immunoblot with the phosphospecific antibodies described. The total amount of STIM1 was evaluated with a non-phosphospecific STIM1 antibody (total STIM1); ERK1/2 activation was monitored with an anti-phospho (pThr202/pTyr204) ERK1/2 antibody. Loading control was monitored with a total anti-ERK1/2 antibody (total ERK1/2). Quantification of the phosphorylation level was performed by blot densitometry after subtracting the background for each blot lane, using the Quantity-One software. Blots are representative of four independent experiments with four different lysates; data correspond to the calculated mean \pm s.d. * P <0.05, *** P <0.001 compared with the control (time 0).

These phosphosites are close to the Thr-Arg-Ile-Pro sequence (or TRIP) (Fig. 5A), encompassing amino acids 642–645, a motif which is shared, as a S/TxIP sequence, by several proteins that bind to the microtubule plus-end regulator EB1 (Tamura and Draviam, 2012). Indeed, it is known that STIM1 directly binds to EB1 (Grigoriev et al., 2008), and therefore STIM1 is considered a microtubule plus-end-tracking protein (+TIP). For other +TIPs it

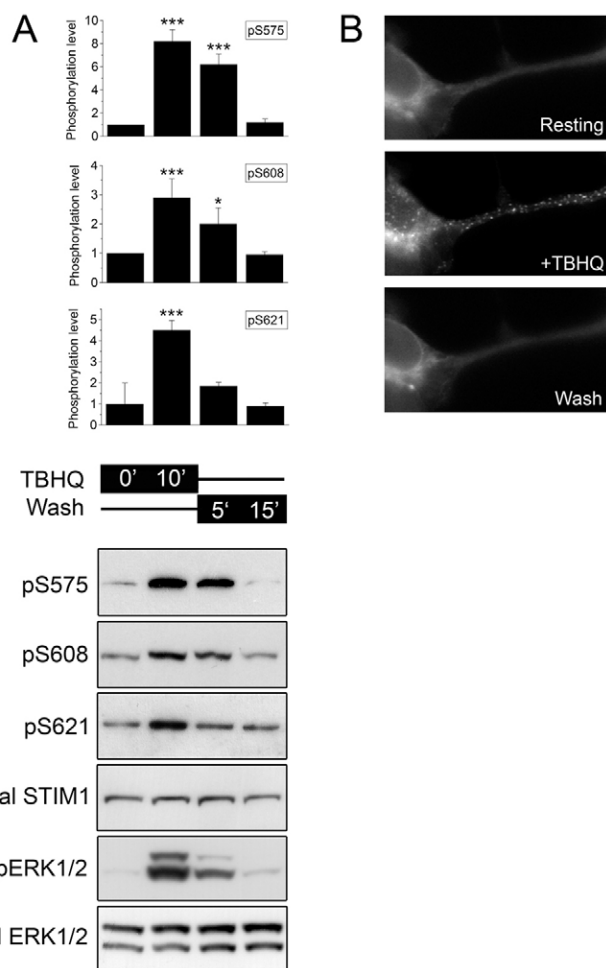


Fig. 3. Reversible phosphorylation of STIM1 at ERK1/2 target sites. (A) HEK293 Flp-In T-REx cells were stably transfected for the inducible expression of STIM1-GFP. Expression of STIM1-GFP was induced by the addition of doxycycline 24 hours prior to the experiment. Cells were incubated in Ca^{2+} -free HBSS with or without the addition of 10 μM TBHQ for 10 minutes. Thereafter, cells were washed (three washing steps) with Ca^{2+} -containing HBSS and incubated in the Ca^{2+} -containing solution for 5 or 15 minutes. Total lysates were used to detect phospho-residues with the phosphospecific antibodies described (labeled as pS575, pS608 and pS621). The total amount of STIM1 was evaluated using an anti-GFP antibody. ERK1/2 activation was monitored with an anti-phospho (pThr202/pTyr204) ERK1/2 antibody (labeled as pERK1/2), and the loading control was monitored with a total anti-ERK1/2 antibody (labeled as total ERK1/2). Quantification of the phosphorylation level was performed as described for Fig. 1. Blots are representative of three independent experiments; data correspond to the calculated mean \pm s.d. * P <0.05, *** P <0.001 compared with the control (TBHQ 0'). (B) HEK293 cells stably expressing STIM1-GFP were treated as described for A, i.e. with 10 μM TBHQ in Ca^{2+} -free HBSS and visualized under epifluorescence microscopy. Thereafter, cells were washed with Ca^{2+} -containing HBSS in order to remove TBHQ. Images were taken every 10 seconds (100 milliseconds/frame) using GFP excitation/emission wavelengths. The initial resting state (top), the clustering of STIM1-GFP after the TBHQ treatment (middle), and the reversal of clustering upon TBHQ washing and Ca^{2+} addition (bottom) are shown. The full movie is provided (supplementary material Movie 1).

has been reported that phosphorylation in the vicinity of the S/TxIP sequence regulates the binding to EB1 (Tamura and Draviam, 2012; Watanabe et al., 2009; Zumbunn et al., 2001). We

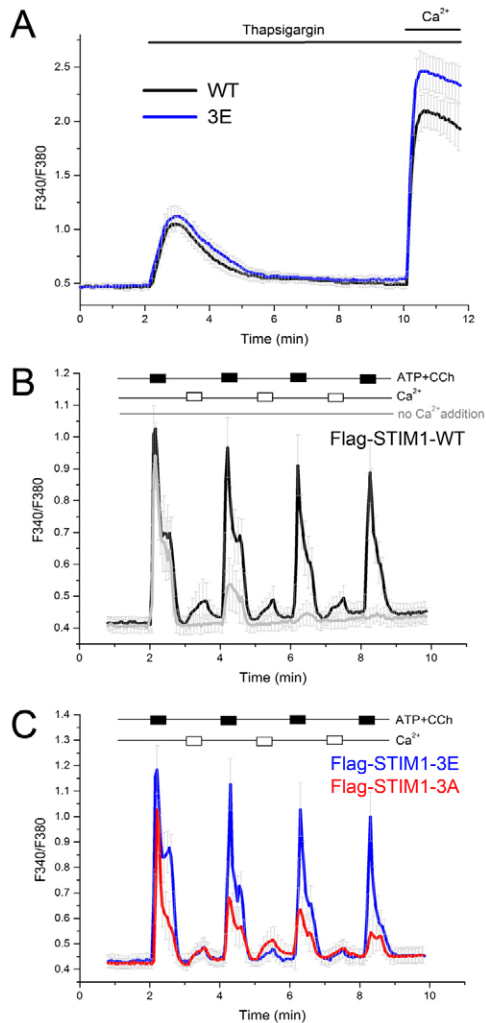


Fig. 4. Ca^{2+} mobilization in HEK293 cells expressing FLAG-STIM1-S/A or FLAG-STIM1-S/E mutants. (A) HEK293 cells stably transfected for the expression of FLAG-STIM1-wild-type (labeled as WT; black line), or FLAG-STIM1^{S575E/S608E/S621E} (labeled as 3E; blue line) were treated with doxycycline for 24 hours prior to the experiment. After 8 hours in serum-free medium, SOCE was evaluated in fura-2-loaded cells after the addition of 1 μM thapsigargin in Ca^{2+} -free HBSS followed by the addition of 2 mM Ca^{2+} . The ratio F340/F380 was monitored by epifluorescence as described in Materials and Methods. (B) Cells expressing FLAG-STIM1 (black line) were challenged by sequential addition of 100 μM ATP plus 100 μM carbachol (ATP+CCh) for 30 seconds in Ca^{2+} -free HBSS, two washing steps with Ca^{2+} -free HBSS, addition of 2 mM Ca^{2+} (Ca^{2+} -containing HBSS), followed by two washing steps with Ca^{2+} -free HBSS. This protocol was repeated three additional times. In parallel, cells expressing FLAG-STIM1 were treated following identical purinergic stimulation in Ca^{2+} -free medium (gray line). In this latter case, no Ca^{2+} was added at any stage. (C) Cells expressing FLAG-STIM1^{S575E/S608E/S621E} (3E; blue line) and cells expressing FLAG-STIM1^{S575A/S608A/S621A} (3A; red line) were challenged by sequential purinergic stimulation as indicated in B. Figures are representative of four independent experiments. For each experiment, performed in duplicate, ~ 40 cells per condition were evaluated. Data are mean \pm s.d.

therefore tested the hypothesis that phosphorylation of STIM1 at ERK1/2 target sites could be regulating the interaction with EB1. To study in depth the STIM1-EB1 interaction in HEK293 cells, we transfected STIM1-GFP-expressing cells with HA-EB1, and

performed a GFP pull-down assay. In parallel, we transfected cells that expressed GFP only with HA-EB1 as a negative control of this co-precipitation assay. Cells were treated with Tg in Ca^{2+} -free medium as described above to induce store depletion, whereas control cells were incubated with Ca^{2+} -containing HBSS. Firstly, we observed a significant decrease of the co-precipitated HA-EB1 from store depleted cells when compared to resting cells (Fig. 5B). We thus confirmed a decrease in STIM1-EB1 binding during store depletion, as had been suggested previously (Grigoriev et al., 2008). Moreover, in cells expressing STIM1^{S575A/S608A/S621A}-GFP, we did not detect any change in the level of co-precipitated HA-EB1 even after the treatment with Tg, suggesting that dephosphorylation of STIM1 at Ser575, Ser608 and Ser621 promoted the binding to EB1. This result is concordant with that observed with wild-type STIM1, for which we found higher binding levels in resting cells, i.e. when STIM1 is dephosphorylated at ERK1/2 target sites (see Fig. 1). Finally, STIM1^{S575E/S608E/S621E}-GFP did not bind to EB1 under any experimental condition, further confirming that phosphorylated STIM1 at ERK1/2 target sites dissociates from EB1, an event observed during store-depletion in wild-type STIM1-expressing cells. In parallel, we monitored the efficient phosphorylation induced by store depletion with a phosphoSer575 antibody (input; bottom blot). Due to the importance of this finding we designed an alternative strategy to study this regulation. We transfected FLAG-STIM1 expressing cells with EB1-GFP and performed a GFP pull-down assay, as described above. As a negative control we used FLAG-peptide (empty) expressing cells transfected with EB1-GFP. As was described above, we observed a weaker binding between STIM1 and EB1 during store depletion (Fig. 5C). This binding was negligible in cells expressing FLAG-STIM1^{S575E/S608E/S621E}, but robust in cells expressing FLAG-STIM1^{S575A/S608A/S621A}, thus confirming our previous finding.

The immunolocalization of endogenous EB1 in cells expressing STIM1-GFP was then analysed by confocal microscopy, revealing that STIM1-EB1 colocalization dropped significantly after store depletion triggered by Tg (Fig. 6), in agreement with the results shown in Fig. 5. However, STIM1-EB1 dissociation was not evident for the S/A mutant (STIM1^{S575A/S608A/S621A}-GFP) under store depletion, whereas the colocalization of EB1 and STIM1^{S575E/S608E/S621E}-GFP was similar to that observed for wild-type STIM1 in cells under store depletion conditions, i.e. it remained at low levels. In this regard, a previous report suggested that dissociation of STIM1 from EB1 is required for the multimerization-dependent activation of STIM1 (Sampieri et al., 2009). We therefore monitored the kinetics of STIM1 multimerization in response to store-depletion in cells expressing STIM1-GFP, STIM1^{S575A/S608A/S621A}-GFP, or STIM1^{S575E/S608E/S621E}-GFP. The results indicated that STIM1 multimerization was faster when residues Ser575, Ser608 and Ser621 were mutated to Glu, mimicking Ser phosphorylation (Fig. 7A). On the contrary, Ser to Ala mutation significantly reduced this kinetics compared to wild-type STIM1. Thus, our results confirmed that phosphorylation of ERK1/2 target sites modulates STIM1 multimerization, an explanation for the inhibitory effect of dephosphorylation of STIM1 on SOCE. To fully confirm this possibility we expressed wild-type STIM1 constitutively bound to EB1-GFP in HEK293 cells. STIM1-EB1-GFP was incapable of forming puncta under store depletion conditions (Fig. 7B), arguing for a significant role of STIM1-EB1 dissociation in STIM1 multimerization. Because the

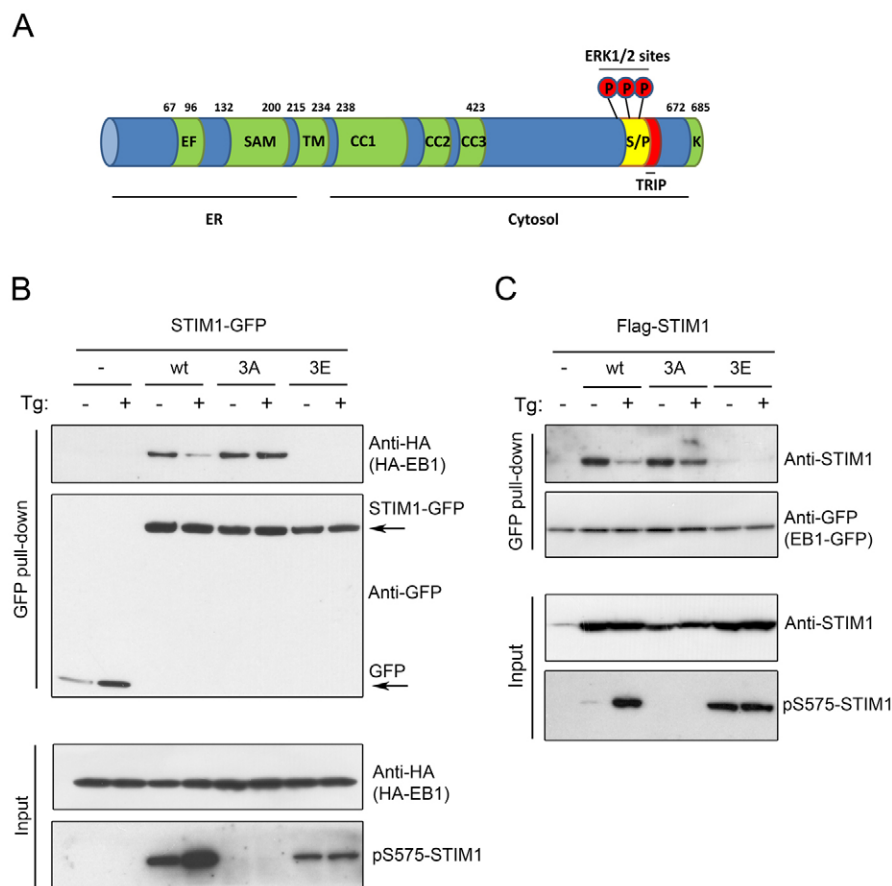


Fig. 5. STIM1 phosphorylation at Ser575, Ser608 and Ser621 regulates the binding to EB1. (A) Scheme showing STIM1 domains: EF, Ca²⁺-binding EF-hand; SAM, sterile α motif; TM, transmembrane; CC1–CC3, coiled-coil domains 1–3; S/P, Ser/Pro-rich domain; TRIP, Thr⁶⁴²-Arg⁶⁴³-Ile⁶⁴⁴-Pro⁶⁴⁵ sequence; K, Lys-rich domain. The scheme indicates the relative position of ERK1/2 target sites (Ser575, Ser608 and Ser621). (B) HEK293 cells stably expressing STIM1-GFP (wild-type, S575A/S608A/S621A or S575E/S608E/S621E; labeled as wt, 3A and 3E, respectively) were transfected for transient expression of HA-EB1. At 24 hours after transfection, cells were incubated in Ca²⁺-containing HBSS (–Tg) or in Ca²⁺-free HBSS with 1 μ M thapsigargin for 10 minutes (+Tg), as for Fig. 1. GFP-tagged STIM1 from these cells was pulled-down with GFP-Trap using low ionic strength to keep native molecular complexes intact. The level of EB1 bound to STIM1 was evaluated by immunoblot using an anti-HA antibody (upper panel), and the level of pulled-down STIM1-GFP was evaluated with an anti-GFP antibody. As a negative control, we used cells overexpressing GFP (without STIM1-GFP, first two lanes). The total amount of HA-EB1 in every experimental condition is shown (input). Finally, to test STIM1 activation by store depletion we monitored phospho-Ser575-STIM1 in this experiment. Note the increase of signal (level of pSer575) in Tg-treated cells for STIM1 wild-type. (C) HEK293 cells stably expressing FLAG-STIM1 (wt, 3A or 3E) were transfected for transient expression of EB1-GFP. As in B, 24 hours after transfection cells were incubated in Ca²⁺-containing HBSS (–Tg) or in Ca²⁺-free HBSS with thapsigargin for 10 minutes (+Tg). EB1-GFP was pulled-down with GFP-Trap, and the level of FLAG-STIM1 bound to EB1-GFP was evaluated by immunoblotting using an anti-STIM1 antibody (upper panel). The level of pulled-down EB1-GFP was evaluated with an anti-GFP antibody. As a negative control we used cells overexpressing FLAG-peptide, transfected with EB1-GFP (first lane). The total amount of FLAG-STIM1 in every experimental condition is shown (input). The low level of STIM1 observed in cells overexpressing FLAG-peptide (first lane) corresponds to endogenous STIM1. As for A, we tested STIM1 phosphorylation with a phosphospecific anti-STIM1 antibody (pS575-STIM1). Blots are representative of three independent experiments with three different cultures.

mutation of residues Ile-Pro to Asn-Asn in the sequence S/TxIP abolishes the binding to EB1 (Honnappa et al., 2009) (supplementary material Fig. S1), we studied the multimerization of STIM1^{I644N/P645N}-GFP in cells under store depletion conditions (Fig. 7B). The results confirmed the hypothesis that the binding to EB1, and therefore to microtubules, disables STIM1 capacity to form puncta, whereas the release from EB1 enables STIM1 to aggregate in clusters. We also confirmed the requirement of the dissociation of the STIM1-EB1 complex to trigger SOCE because FLAG-STIM1-EB1 was unable to activate Ca²⁺ entry, whereas fully dissociated STIM1 (FLAG-STIM1^{I644N/P645N}) behaved similarly to wild-type STIM1 and to STIM1^{S575E/S608E/S621E}

when activating SOCE (Fig. 7C). Consequently we confirmed that a reversible mechanism is required to trigger STIM1-EB1 dissociation when Ca²⁺ entry needs to be activated. The diminished Ca²⁺ entry found in FLAG-STIM1^{S575A/S608A/S621A}-expressing cells together with the stronger binding of dephosphorylated STIM1 to EB1, the finding that the STIM1-EB1 complex is modulated by phosphorylation of STIM1 at ERK1/2 sites, and the finding that constitutively bound STIM1 to EB1 is unable to activate SOCE suggest that phosphorylation of STIM1 constitutes a major mechanism for regulating Ca²⁺ entry through the modulation of the EB1-STIM1 complex.

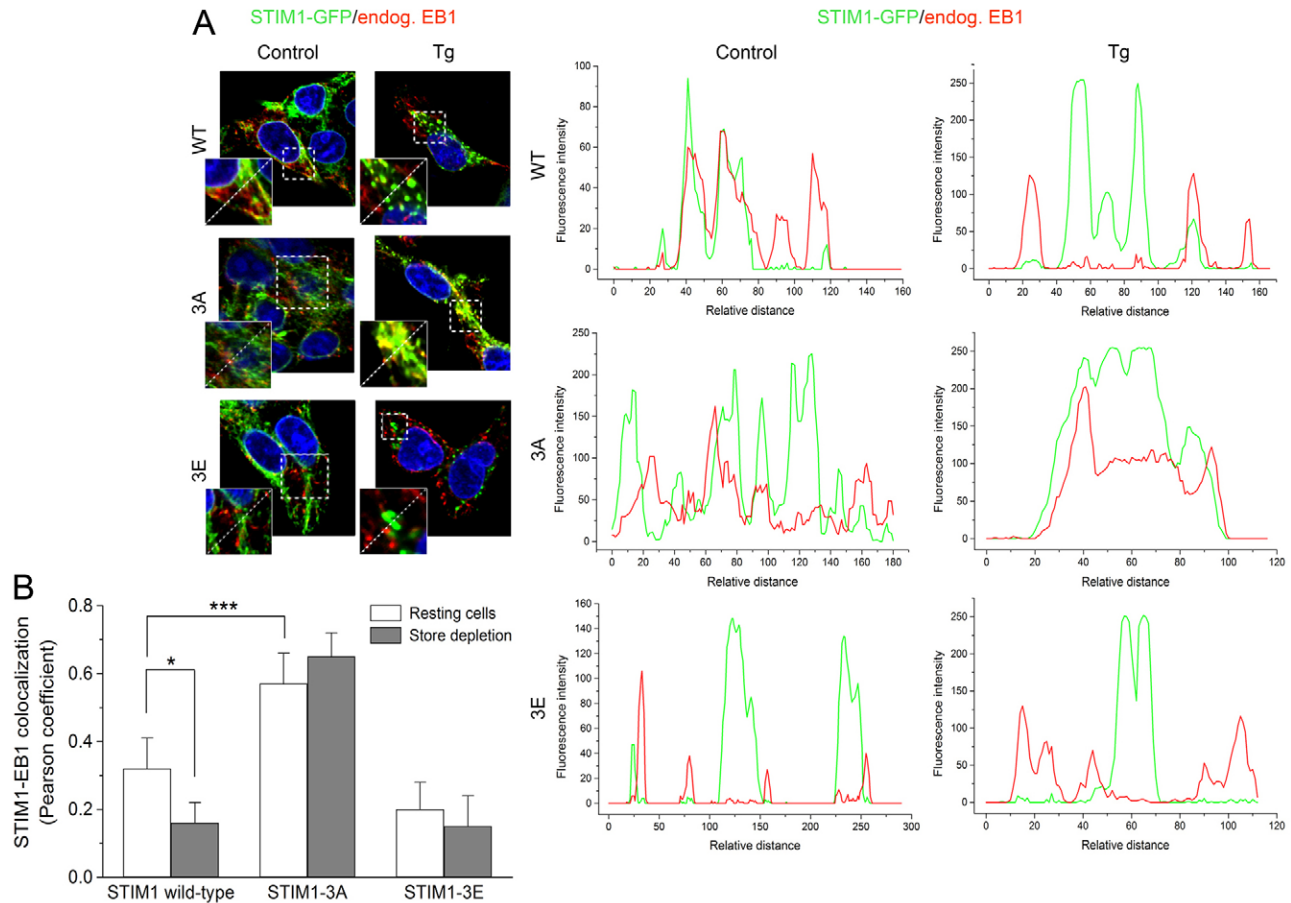


Fig. 6. STIM1-EB1 colocalization in HEK293 cells. (A) Left: Cells expressing STIM1-GFP (wild-type, S575A/S608A/S621A or S575E/S608E/S621E; labeled as WT, 3A and 3E, respectively) were incubated in Ca^{2+} -containing HBSS (control), or in Ca^{2+} -free HBSS with thapsigargin for 10 minutes (+Tg), as described. After fixation, endogenous EB1 was immunolocalized with an anti-EB1 monoclonal antibody and a secondary anti-mouse IgG antibody labeled with Alexa Fluor 633. Hoechst 33342 nuclear counterstain is shown in blue. Selected areas were analyzed to show the line intensity profile for the diagonal line (from upper right corner to bottom left corner). Images are representative fields from three different experiments, performed in triplicate. Right: Line profile of fluorescent intensities to show colocalization of STIM1-GFP (green) and endogenous EB1 (red) in resting cells or under store depletion conditions. (B) STIM1-EB1 colocalization was evaluated with the Pearson correlation coefficient using a minimum of 12 frames per experimental condition from three independent cultures. * $P < 0.05$, *** $P < 0.001$.

Discussion

This work has demonstrated the close relationship between Ca^{2+} store depletion, ERK1/2 activation and STIM1 phosphorylation. Conversely, Ca^{2+} entry is linked to ERK1/2 deactivation and STIM1 dephosphorylation. ERK1/2 activation drives STIM1 phosphorylation at Ser575, Ser608 and Ser621 in HEK293 cells, as was demonstrated here with the use of phosphospecific antibodies against phosphorylated residues. As we reported previously, no other sites within STIM1 are found to be phosphorylated *in vitro* by ERK1/2 (Pozo-Guisado et al., 2010). Because phosphorylated STIM1 efficiently supports activation of SOCE, whereas dephosphorylated STIM1 is unable to activate Ca^{2+} entry, our findings strongly suggest that reversible phosphorylation of STIM1 is a mechanism that controls Ca^{2+} -entry. In those signaling pathways where ERK1/2 is not activated, an insufficient phosphorylation of STIM1 may decelerate or delay Ca^{2+} entry, unless other kinases phosphorylate STIM1 at these sites. A large number of growth factors, cytokines and hormones modulate different signaling pathways, including the MAPK pathway. In these cases, the

phosphorylation of STIM1 would have a significant impact on cell signaling by means of the activation of Ca^{2+} entry through SOCs. Thus, our results provide a new potential mediator, STIM1, in those signaling pathways where MAPK and Ca^{2+} entry are involved. This would be the case for platelet activation (Elvers et al., 2012) and myoblast differentiation (Lee et al., 2012), although the hypothesis has not been fully confirmed in those cell types due to the lack of phosphospecific antibodies against those sites. Because our work has focused on the molecular mechanism underlying the regulation of STIM1 activity by phosphorylation, the involvement of STIM1 phosphorylation in signaling pathways and physiological events mediated by ERK1/2 will require further study in the future.

STIM1 is transported through ER tubules by a mechanism dependent on EB1, which is a well known regulator of growing microtubule ends. Indeed, STIM1 directly binds to EB1 and, to a lesser extent, to EB2 and EB3, so that STIM1 is regarded as a microtubule plus-end-tracking protein (+TIP) (Grigoriev et al., 2008). Although the interaction between STIM1 and microtubules has been proven, its regulation is still a point of

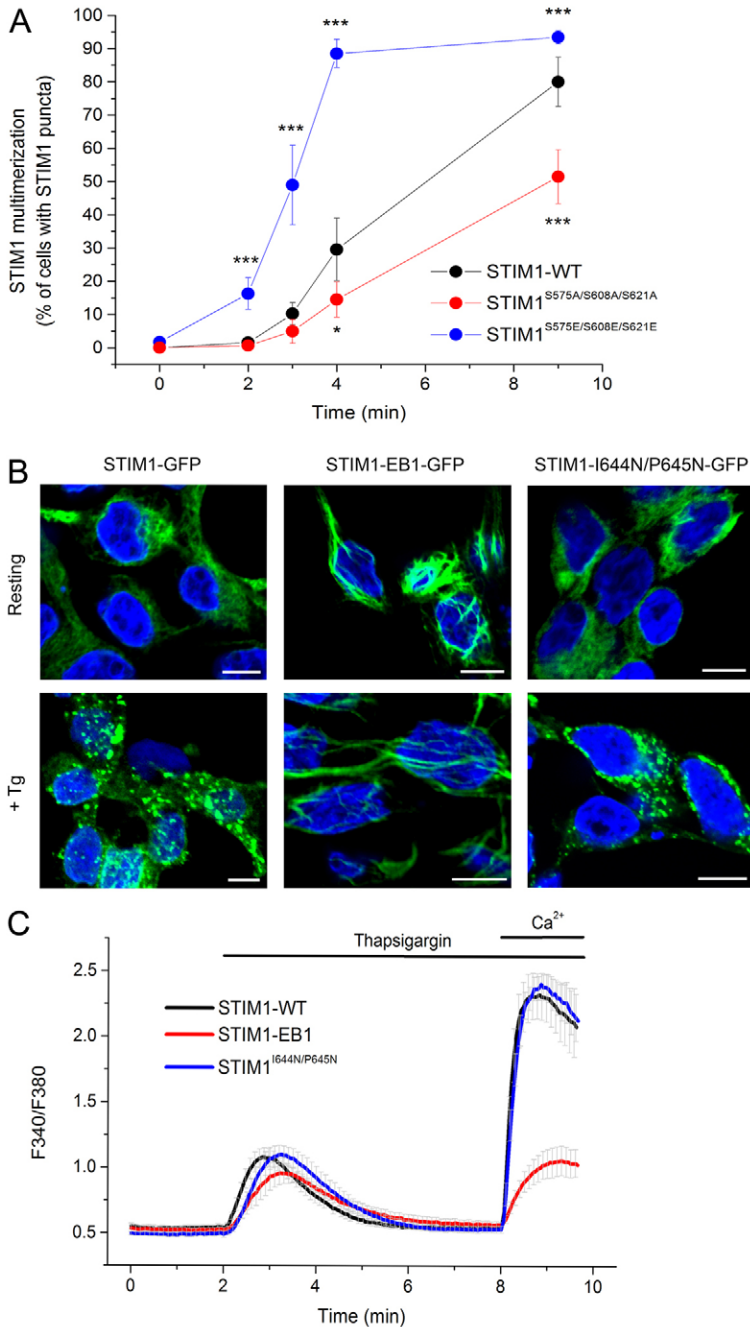


Fig. 7. EB1-dependent multimerization of STIM1. (A) HEK293 cells expressing STIM1-GFP (wild-type, S575A/S608A/S621A or S575E/S608E/S621E) were incubated in Ca^{2+} -free HBSS with 10 μM TBHQ at 30°C. At the indicated times, cells were fixed in 4% freshly made paraformaldehyde and counterstained with Hoechst 33342 for 5 minutes. The percentage of cells with patent STIM1 multimerization during store-depletion treatment was calculated from a minimum of eight different fields (>200 cells per condition) from three independent cultures. * $P < 0.05$, *** $P < 0.001$ compared with STIM1 wild-type. (B) HEK293 cells expressing STIM1-GFP (wild-type), STIM1-EB1-GFP or STIM1^{I644N/P645N}-GFP were incubated in Ca^{2+} -free HBSS with 1 μM thapsigargin for 10 minutes. Confocal images were taken before thapsigargin addition (resting), and at the end of the experiment (+Tg) to show distribution of STIM1. Representative images from three different cultures performed in triplicate. (C) HEK293 cells transfected for the expression of FLAG-STIM1-wild-type (STIM1-WT; black line), FLAG-STIM1-EB1 (STIM1-EB1; blue line), or FLAG-STIM1^{I644N/P645N} (STIM1^{I644N/P645N}; red line) were treated with doxycycline for 24 hours prior to the experiment. SOCE was evaluated in fura-2-loaded cells after the addition of 1 μM thapsigargin in Ca^{2+} -free HBSS followed by the addition of 2 mM Ca^{2+} . The figure shows representative traces of three independent experiments. For each experiment, performed in duplicate, ~30 cells per condition were evaluated. Data are mean \pm s.d. Scale bars: 5 μm .

intense debate. It has been reported that EB1-STIM1 colocalization behaves differently in MRC5-SV fibroblasts and HeLa cells (Grigoriev et al., 2008). Whereas STIM1 colocalized with EB1 even after store depletion in HeLa cells, it moved independently from EB1 in MRC5-SV fibroblasts under the same conditions, and it was concluded that the association of STIM1 to microtubules is not required for the activation of SOCE (Grigoriev et al., 2008). Other authors have found, however, that the treatment of HEK293 cells with nocodazole, an inhibitor of microtubule polymerization, leads to the inhibition of SOCE (Smyth et al., 2007), suggesting a positive modulatory role of STIM1-microtubule association. Subsequently, Sampieri et al. found that STIM1 dissociation from EB1 is a prerequisite to

initiate puncta formation and the activation of ORAI1 (Sampieri et al., 2009). However, the mechanism that induces the dissociation of STIM1-EB1 required for proper SOCE activation is unknown. Several pieces of evidence led us to study phosphorylation as a possible mechanism that regulates this important association: (i) it was suggested that the Ser/Pro domain of STIM1 is required for puncta formation in response to store depletion, because deletion of the Ser/Pro domain impaired the formation of puncta and therefore was unable to support SOCE (Baba et al., 2006); (ii) STIM1 binds to EB1 through a sequence located close to this specific domain (Honnappa et al., 2009); (iii) the binding of other +TIPs to EB1 is regulated by phosphorylation (Kumar et al., 2009; Watanabe et al., 2009;

Zumbrunn et al., 2001); and (iv) STIM1 is phosphorylated in the vicinity of the sequence that serves as binding motif to EB1 (Poza-Guisado et al., 2010). We therefore hypothesized that phosphorylation of STIM1 at ERK1/2 sites might be controlling the dissociation of STIM1 from EB1. Indeed, the present work has provided solid evidence that phosphorylation of STIM1 at ERK1/2 target sites triggers the dissociation of STIM1 from EB1, which is required to activate SOCE, whereas constitutive dephosphorylation maintains this binding even under store depletion conditions. Our results are in agreement with previous reports on other +TIPs, such as the cytoplasmic linker-associated proteins (CLASPs)-(Kumar et al., 2009), APC (Nathke, 2004), and MCAK (Andrews et al., 2004), which are all phosphorylated in the vicinity of the S/TxIP sequence, regulating how they interact with microtubules. In all cases, as also with STIM1, sequences flanking the S/TxIP motif contain many Pro, Ser, and basic residues, leading to a net positive charge in the surroundings of this binding domain to EB1. This observation can explain why phosphorylation in the vicinity of this sequence negatively regulates the localization of +TIPs to microtubule ends, although the precise mechanism underlying this regulation is not known. Our conclusions do not rule out the possibility that other phospho-sites can trigger different actions, as occurs for CLASPs, where differential phosphorylation profile determines whether CLASPs track plus ends or associates along microtubules (Kumar et al., 2009). This may be the case for STIM1, because phosphorylation at ERK1/2 sites dissociates the protein from EB1 and promotes SOCE (data shown here), but other phospho-residues have been related to the inhibition of SOCE during mitosis (Smyth et al., 2009), although the molecular details of this inhibition are unknown. In addition, it is possible that other posttranslational modifications may have an impact on phosphorylation of STIM1 therefore modulating its function. In this regard, the modification of STIM1 at Ser/Thr residues with O-linked *N*-acetylglucosamine (O-GlcNAcylation) attenuates STIM1 multimerization in neonatal cardiomyocytes, leading to SOCE inhibition (Zhu-Mauldin et al., 2012). Also, these authors reported that increased STIM1 O-GlcNAcylation alters the phospho-regulation of STIM1, therefore suggesting a relationship between both posttranslational modifications.

To summarize, our results demonstrate that STIM1-EB1 binding is regulated by phosphorylation of STIM1 at ERK1/2 sites. STIM1 becomes phosphorylated at ERK1/2 sites during store depletion, and this phosphorylation favours STIM1-EB1 dissociation, as demonstrated by the S/A and S/E mutations shown here. This conclusion can explain why S/A mutation at ERK1/2 target sites significantly reduces SOCE, similarly to what was observed here when STIM1 remained constitutively bound to EB1. The combination of all these observations allows us to propose a model in which dephosphorylated STIM1, at Ser575, Ser608 and Ser621 remains bound to EB1 in resting cells, but releases from EB1 when it becomes phosphorylated under store depletion conditions (Fig. 8). This model fits well with the proposal that STIM1 forms comet-like structures when it binds to EB1 in non-stimulated cells but is able to form immobile STIM1 clusters at ER-PM junctions, whereas EB1-positive microtubule ends are unaffected by Tg (Grigoriev et al., 2008; Honnappa et al., 2009). Phosphorylated STIM1 leads to SOCE activation, and the subsequent Ca^{2+} store refilling is accompanied by dephosphorylation of STIM1, which supports the binding back to EB1. Although further investigation is required to determine

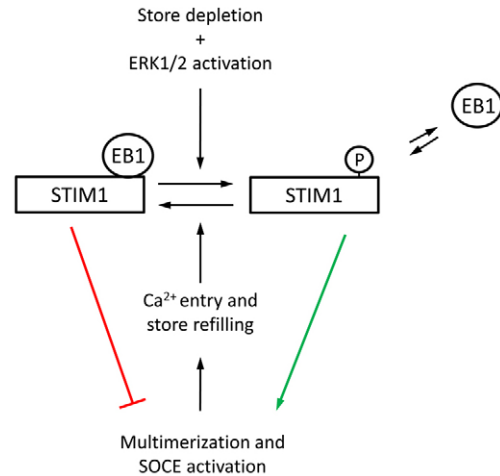


Fig. 8. Regulation of SOCE by phosphorylation of STIM1 at ERK1/2 sites. Ca^{2+} release from the ER leads to a decreased intraluminal Ca^{2+} concentration and to ERK1/2 activation. ERK1/2 phosphorylates STIM1 at Ser575, Ser608 and Ser621, triggering the dissociation from EB1. EB1-dissociated STIM1 then aggregates to form puncta, which is a prior step for the activation of SOC channels. Refilling of Ca^{2+} stores facilitates STIM1 dephosphorylation, thus enhancing STIM1-EB1 binding to avoid prolonged STIM1-dependent activation of SOC channels.

whether different combinations of phospho-residues found in STIM1 trigger differential responses, our results demonstrate that reversible phosphorylation of STIM1 at ERK1/2 target sites constitutes a major molecular mechanism that regulates STIM1-EB1 interaction, a mechanism that controls SOCE activation.

Materials and Methods

Materials

Doxycycline, Tween 20 and DMSO were obtained from Sigma; Flp-In T-Rex HEK293 cells, zeocin, blasticidin, NuPAGE Bis-Tris gels were from Life Technologies; hygromycin B was from Invivogen; PD184352 and PD0325901 were from Axon Medchem; Nonidet P40 was from Fluka; fura-2-acetoxymethyl ester (fura-2-AM) was from Calbiochem; thapsigargin (Tg) and 2,5-di-(*tert*-butyl)-1,4-benzohydroquinone (TBHQ) were from Abcam Biochemicals; GFP-Trap resin was from Chromotek; and polyethylenimine was purchased from Polysciences, Inc.

Antibodies

The following phosphospecific antibodies were raised in sheep and affinity purified on the appropriate antigen by the Division of Signal Transduction Therapy (DSTT), University of Dundee (Dundee, UK): the STIM1 phospho-Ser575 was raised against a phosphopeptide encompassing residues 567–581 of mouse STIM1 (LVEKLPDSpSPALAKK). The STIM1 phospho-Ser608 was raised against a phosphopeptide encompassing residues 601–614 of mouse STIM1 (PSVPPGGpSPLLDSS) plus addition of one Arg residue at N-terminal and two Arg residues at C-terminal to promote peptide solubility. The STIM1 phospho-Ser621 was raised against a phosphopeptide encompassing residues 614–628 of mouse STIM1 (SHSLSPSpSPDPDTPS) plus the addition of two Arg residues at N-terminal and two Arg residues at C-terminal to promote peptide solubility.

The following antibodies were purchased from Cell Signaling Technology: anti-ERK1/2 (total), anti-ERK1/2 phospho-Thr202/Tyr204 and anti-GFP antibody, produced in rabbit. The anti-HA antibody, produced in rabbit, was from Sigma. Mouse monoclonal anti-EB1 was from BD Transduction Laboratories. The rabbit polyclonal anti-STIM1 antibody was from ProSci.

DNA constructs

Mouse Stim1 (accession number NM_009287) was cloned as a *Bam*HI-*Not*I insert into a pcDNA5/FRT/TO vector (Life Technologies), carrying an N-terminal FLAG (DYKDDDDK) or C-terminal GFP tag. Mouse Eb1 (accession number NM_007896) was cloned as an *Xho*I-*Sac*II insert into pEGFP-N1 (Clontech) or as an *Eco*RI-*Not*I insert into pCMV HA-1 (this vector was a kind gift from Dr James Hastie, Division of Signal Transduction Therapy, University of Dundee,

UK). Mutagenesis was performed using the QuikChange site-directed mutagenesis method (Agilent). To generate the STIM1-EB1-GFP protein, Eb1 cDNA was cloned within the *NotI* site of the pcDNA5/FRT/TO vector carrying STIM1-GFP. DNA constructs used for transfection were purified from *E. coli* DH5 α using Qiagen Plasmid kits according to the manufacturer's protocol. All DNA constructs were verified by DNA sequencing using BigDye Terminator v3.1 cycle sequencing protocol (Life Technologies) on 3130 Genetic Analyzer (Life Technologies) at the DNA Sequencing Facility of STAB, University of Extremadura, Spain.

General methods and solutions

The lysis buffer used for HEK293 cells was 50 mM Tris-HCl (pH 7.5), 1 mM EGTA, 1 mM EDTA, 1% (w/v) Nonidet P40, 1 mM sodium orthovanadate, 50 mM sodium fluoride, 5 mM sodium pyrophosphate, 0.27 M sucrose, 0.1% (v/v) 2-mercaptoethanol, 1 mM benzamide, and 0.1 mM PMSF. Clarification of samples was performed after lysis with 1 ml of ice-cold lysis buffer/dish and centrifugation at 4°C for 15 minutes at 20,000 g. Buffer A was 50 mM Tris-HCl (pH 7.5), 0.1 mM EGTA, and 0.1% (v/v) 2-mercaptoethanol. LDS sample buffer contained 50 mM Tris-HCl (pH 6.8), 2% (w/v) LDS, 10% (v/v) glycerol, 0.005% (w/v) bromophenol blue, and 10 mM DTT. TBS-T buffer was Tris-HCl (pH 7.5), 0.15 M NaCl and 0.5% (v/v) Tween 20. Protein concentration was determined using the Bradford reagent (Bio-Rad).

Culture of HEK293 cells

Flp-In T-REx HEK293 cells able to inducibly express tagged STIM1 were generated as reported previously (Pozo-Guisado et al., 2010). Stably transfected cells (resistant to hygromycin and blasticidin) were cultured in Dulbecco's modified Eagle's medium (DMEM) with 10% (v/v) foetal bovine serum, 2 mM L-glutamine, 100 U/ml penicillin, 0.1 mg/ml streptomycin, 100 μ g/ml hygromycin B, and 15 μ g/ml blasticidin in a humidified atmosphere of air/CO₂ at 37°C. Cells were treated with 1 μ g/ml doxycycline for 24 hours before assays to induce expression of tagged STIM1, as we reported previously (Pozo-Guisado et al., 2010). Transfection of cells with additional DNA constructs was performed with 1–2 μ g plasmid DNA and polyethylenimine in serum-containing medium, 24 hours prior to the beginning of the experiments.

Pull-down of GFP-tagged proteins

GFP-tagged STIM1 or EB1 were purified as indicated previously (Pozo-Guisado et al., 2010). Briefly, equilibrated GFP-Trap beads were added to cell lysates and incubated from samples by incubating 8 μ l of GFP-Trap beads with 3 mg of the clarified lysate for STIM1-GFP pull-down, or 5 μ l of beads with 0.5 mg of the lysate for EB1-GFP pull-down. In both cases, lysates were incubated with the beads for 1 hour at 4°C. The beads were washed twice with 1 ml lysis buffer containing 0.15 M NaCl and twice with buffer A. Proteins were eluted from the GFP-Trap beads by the addition of 7 μ l NuPAGE-LDS sample buffer to the beads. Eluted proteins were reduced by the addition of 10 mM DTT followed by heating at 90°C for 4 minutes.

Cytosolic free calcium concentration

Cytosolic free calcium concentration, [Ca²⁺]_i, was measured basically as described elsewhere (Gutierrez-Martin et al., 2005; Pozo-Guisado et al., 2010), in fura-2-AM-loaded cells, using an inverted microscope Nikon TE2000-U equipped with micro-incubation platform DH-40i (Warner Instruments). All measurements were performed at 35°C (heater controller TC-324B, Warner Instruments). Depletion of Ca²⁺ stores was triggered by incubating cells with 1 μ M Tg or 10 μ M TBHQ in Ca²⁺-free HBSS with the following composition: 138 mM NaCl; 5.3 mM KCl; 0.34 mM Na₂HPO₄; 0.44 mM KH₂PO₄; 4.17 mM NaHCO₃; 4 mM Mg²⁺ (pH 7.4). SOCE was measured by monitoring the increase of the [Ca²⁺]_i after the addition of 2 mM CaCl₂ to the Tg-containing medium. In those experiments conducted for the study of SOCE reversion, TBHQ-treated cells were washed with HBSS containing 1.26 mM CaCl₂.

Immunostaining and microscopy

Immunolocalization of endogenous EB1 was performed in STIM1-GFP-expressing HEK293 cells fixed with methanol for 15 minutes at –20°C, followed by paraformaldehyde (4% in PBS for 15 minutes at room temperature). Permeabilization was performed with 0.2% Triton X-100 and blocking with 3% skin gelatin in PBS plus Tween 0.2% for 30 minutes at room temperature. Cells were incubated overnight at 4°C with the mouse monoclonal anti-EB1 antibody at 1:200 dilution. Anti-mouse IgG labeled with Alexa Fluor 633 was used as a secondary antibody (diluted 1:250, 30 minutes at room temperature). Covers were mounted onto glass slides with hydromount after nuclei counterstaining with 1 μ g/ml Hoechst 33342. Confocal microscopy was performed at the Cytomics Unit of STAB of the University of Extremadura. Images of fixed cells were taken on a Fluoview 1000 Confocal microscope (Olympus) with a 60 \times NA 1.45 oil immersion objective. Image analysis to evaluate the line profile of fluorescence intensities was performed with the FV10-ASW software. Co-localization was evaluated using the Pearson correlation coefficient with the FV10-ASW software.

STIM1-GFP clustering was also monitored by visualization of paraformaldehyde-fixed cells on a Nikon TE2000-U inverted epifluorescence microscope. Cells with multimerization of STIM1-GFP under visualization with a 40 \times (NA 0.9) objective were considered positive for this calculation.

Statistical analysis

Statistical analyses were done by the one-way analysis of variance (ANOVA). Differences between groups of data were statistically significant for $P < 0.05$. Values are represented as follows: * $P < 0.05$, ** $P < 0.01$ and *** $P < 0.001$.

Acknowledgements

We thank the protein and antibodies production teams of the Division of Signal Transduction Therapy (DSTT), University of Dundee (UK), co-ordinated by James Hastie and Hilary McLauchlan, for the production of phosphospecific antibodies against Ser575, Ser608 and Ser621. We acknowledge the work carried out by the staff of the Bioscience Applied Techniques Facility, University of Extremadura, for their support with confocal microscopy.

Author contributions

E.P.-G. and F.J.M.-R. designed the project. E.P.-G., V.C.-R., P.T.-M., A.M.L.-G. and F.J.M.-R. designed and performed the experiments. All authors interpreted data. E.P.-G. and F.J.M.-R. drafted the article. All authors revised the manuscript and approved the final version.

Funding

This work was supported by the Spanish Ministerio de Economía y Competitividad [grant number BFU2011-22798] and the European Social Fund. P.T.-M. and A.L.-G. were supported by predoctoral fellowships from Gobierno de Extremadura [grant number PD10081], and Ministerio de Economía y Competitividad [grant number BES-2012-052061].

Supplementary material available online at

<http://jcs.biologists.org/lookup/suppl/doi:10.1242/jcs.125054/-/DC1>

References

- Andrews, P. D., Ovechkina, Y., Morrice, N., Wagenbach, M., Duncan, K., Wordeman, L. and Swedlow, J. R. (2004). Aurora B regulates MCAK at the mitotic centromere. *Dev. Cell* **6**, 253–268.
- Baba, Y., Hayashi, K., Fujii, Y., Mizushima, A., Watarai, H., Wakamori, M., Numaga, T., Mori, Y., Iino, M., Hikida, M. et al. (2006). Coupling of STIM1 to store-operated Ca²⁺ entry through its constitutive and inducible movement in the endoplasmic reticulum. *Proc. Natl. Acad. Sci. USA* **103**, 16704–16709.
- Bain, J., Plater, L., Elliott, M., Shpiro, N., Hastie, C. J., McLauchlan, H., Klevernic, I., Arthur, J. S., Alessi, D. R. and Cohen, P. (2007). The selectivity of protein kinase inhibitors: a further update. *Biochem. J.* **408**, 297–315.
- Bakowski, D., Glitsch, M. D. and Parekh, A. B. (2001). An examination of the secretion-like coupling model for the activation of the Ca²⁺ release-activated Ca²⁺ current I(CRAC) in RBL-1 cells. *J. Physiol.* **532**, 55–71.
- Elvers, M., Herrmann, A., Seizer, P., Münzer, P., Beck, S., Schönberger, T., Borst, O., Martin-Romero, F. J., Lang, F., May, A. E. et al. (2012). Intracellular cyclophilin A is an important Ca(2+) regulator in platelets and critically involved in arterial thrombus formation. *Blood* **120**, 1317–1326.
- Feske, S., Gwack, Y., Prakriya, M., Srikanth, S., Puppel, S. H., Tanasa, B., Hogan, P. G., Lewis, R. S., Daly, M. and Rao, A. (2006). A mutation in Orai1 causes immune deficiency by abrogating CRAC channel function. *Nature* **441**, 179–185.
- Grigoriev, I., Gouveia, S. M., van der Vaart, B., Demmers, J., Smyth, J. T., Honnappa, S., Splinter, D., Steinmetz, M. O., Putney, J. W., Jr, Hoogenraad, C. C. et al. (2008). STIM1 is a MT-plus-end-tracking protein involved in remodeling of the ER. *Curr. Biol.* **18**, 177–182.
- Gutierrez-Martin, Y., Martin-Romero, F. J. and Henao, F. (2005). Store-operated calcium entry in differentiated C2C12 skeletal muscle cells. *Biochim. Biophys. Acta* **1711**, 33–40.
- Honnappa, S., Gouveia, S. M., Weisbrich, A., Damberger, F. F., Bhavesh, N. S., Jawhari, H., Grigoriev, I., van Rijssel, F. J., Buey, R. M., Lawera, A. et al. (2009). An EB1-binding motif acts as a microtubule tip localization signal. *Cell* **138**, 366–376.
- Kass, G. E., Duddy, S. K., Moore, G. A. and Orrenius, S. (1989). 2,5-Di-(tert-butyl)-1,4-benzohydroquinone rapidly elevates cytosolic Ca²⁺ concentration by mobilizing the inositol 1,4,5-trisphosphate-sensitive Ca²⁺ pool. *J. Biol. Chem.* **264**, 15192–15198.
- Korzeniowski, M. K., Manjarrés, I. M., Varnai, P. and Balla, T. (2010). Activation of STIM1-Orai1 involves an intramolecular switching mechanism. *Sci. Signal.* **3**, ra82.

- Kumar, P., Lyle, K. S., Gierke, S., Matov, A., Danuser, G. and Wittmann, T. (2009). GSK3beta phosphorylation modulates CLASP-microtubule association and lamella microtubule attachment. *J. Cell Biol.* **184**, 895-908.
- Lee, K. P., Yuan, J. P., So, I., Worley, P. F. and Muallem, S. (2010). STIM1-dependent and STIM1-independent function of transient receptor potential canonical (TRPC) channels tunes their store-operated mode. *J. Biol. Chem.* **285**, 38666-38673.
- Lee, H. J., Bae, G. U., Leem, Y. E., Choi, H. K., Kang, T. M., Cho, H., Kim, S. T. and Kang, J. S. (2012). Phosphorylation of Stim1 at serine 575 via netrin-2/Cdo-activated ERK1/2 is critical for the promyogenic function of Stim1. *Mol. Biol. Cell* **23**, 1376-1387.
- Liou, J., Kim, M. L., Heo, W. D., Jones, J. T., Myers, J. W., Ferrell, J. E., Jr and Meyer, T. (2005). STIM is a Ca²⁺ sensor essential for Ca²⁺-store-depletion-triggered Ca²⁺ influx. *Curr. Biol.* **15**, 1235-1241.
- Liou, J., Fivaz, M., Inoue, T. and Meyer, T. (2007). Live-cell imaging reveals sequential oligomerization and local plasma membrane targeting of stromal interaction molecule 1 after Ca²⁺ store depletion. *Proc. Natl. Acad. Sci. USA* **104**, 9301-9306.
- Manji, S. S., Parker, N. J., Williams, R. T., van Stekelenburg, L., Pearson, R. B., Dziadek, M. and Smith, P. J. (2000). STIM1: a novel phosphoprotein located at the cell surface. *Biochim. Biophys. Acta* **1481**, 147-155.
- Muik, M., Frischauf, I., Derler, I., Fahrner, M., Bergsmann, J., Eder, P., Schindl, R., Hesch, C., Polzinger, B., Fritsch, R. et al. (2008). Dynamic coupling of the putative coiled-coil domain of ORA11 with STIM1 mediates ORA11 channel activation. *J. Biol. Chem.* **283**, 8014-8022.
- Muik, M., Fahrner, M., Schindl, R., Stathopoulos, P., Frischauf, I., Derler, I., Plenk, P., Lackner, B., Groschner, K., Ikura, M. et al. (2011). STIM1 couples to ORA11 via an intramolecular transition into an extended conformation. *EMBO J.* **30**, 1678-1689.
- Nathke, I. S. (2004). The adenomatous polyposis coli protein: the Achilles heel of the gut epithelium. *Annu. Rev. Cell. Dev. Biol.* **20**, 337-366.
- Park, C. Y., Hoover, P. J., Mullins, F. M., Bachhawat, P., Covington, E. D., Raunser, S., Walz, T., Garcia, K. C., Dolmetsch, R. E. and Lewis, R. S. (2009). STIM1 clusters and activates CRAC channels via direct binding of a cytosolic domain to Orai1. *Cell* **136**, 876-890.
- Park, C. Y., Shcheglovitov, A. and Dolmetsch, R. (2010). The CRAC channel activator STIM1 binds and inhibits L-type voltage-gated calcium channels. *Science* **330**, 101-105.
- Pozo-Guisado, E., Campbell, D. G., Deak, M., Alvarez-Barrientos, A., Morrice, N. A., Alvarez, I. S., Alessi, D. R. and Martín-Romero, F. J. (2010). Phosphorylation of STIM1 at ERK1/2 target sites modulates store-operated calcium entry. *J. Cell Sci.* **123**, 3084-3093.
- Ribeiro, C. M., Reece, J. and Putney, J. W., Jr (1997). Role of the cytoskeleton in calcium signaling in NIH 3T3 cells. An intact cytoskeleton is required for agonist-induced [Ca²⁺]_i signaling, but not for capacitative calcium entry. *J. Biol. Chem.* **272**, 26555-26561.
- Roos, J., DiGregorio, P. J., Yeromin, A. V., Ohlsen, K., Lioudyno, M., Zhang, S., Safrina, O., Kozak, J. A., Wagner, S. L., Cahalan, M. D. et al. (2005). STIM1, an essential and conserved component of store-operated Ca²⁺ channel function. *J. Cell Biol.* **169**, 435-445.
- Sampieri, A., Zepeda, A., Asanov, A. and Vaca, L. (2009). Visualizing the store-operated channel complex assembly in real time: identification of SERCA2 as a new member. *Cell Calcium* **45**, 439-446.
- Smyth, J. T., DeHaven, W. I., Bird, G. S. and Putney, J. W., Jr (2007). Role of the microtubule cytoskeleton in the function of the store-operated Ca²⁺ channel activator STIM1. *J. Cell Sci.* **120**, 3762-3771.
- Smyth, J. T., DeHaven, W. I., Bird, G. S. and Putney, J. W., Jr (2008). Ca²⁺-store-dependent and -independent reversal of Stim1 localization and function. *J. Cell Sci.* **121**, 762-772.
- Smyth, J. T., Petranka, J. G., Boyles, R. R., DeHaven, W. I., Fukushima, M., Johnson, K. L., Williams, J. G. and Putney, J. W., Jr (2009). Phosphorylation of STIM1 underlies suppression of store-operated calcium entry during mitosis. *Nat. Cell Biol.* **11**, 1465-1472.
- Soboloff, J., Spassova, M. A., Tang, X. D., Hewavitharana, T., Xu, W. and Gill, D. L. (2006). Orai1 and STIM1 reconstitute store-operated calcium channel function. *J. Biol. Chem.* **281**, 20661-20665.
- Tamura, N. and Draviam, V. M. (2012). Microtubule plus-ends within a mitotic cell are 'moving platforms' with anchoring, signalling and force-coupling roles. *Open. Biol.* **2**, 120132.
- Vig, M., Peinelt, C., Beck, A., Koomoa, D. L., Rabah, D., Koblan-Huberson, M., Kraft, S., Turner, H., Fleig, A., Penner, R. et al. (2006). CRACM1 is a plasma membrane protein essential for store-operated Ca²⁺ entry. *Science* **312**, 1220-1223.
- Wang, Y., Deng, X., Mancarella, S., Hendron, E., Eguchi, S., Soboloff, J., Tang, X. D. and Gill, D. L. (2010). The calcium store sensor, STIM1, reciprocally controls Orai and CaV1.2 channels. *Science* **330**, 105-109.
- Watanabe, T., Noritake, J., Kakeno, M., Matsui, T., Harada, T., Wang, S., Itoh, N., Sato, K., Matsuzawa, K., Iwamatsu, A. et al. (2009). Phosphorylation of CLASP2 by GSK-3beta regulates its interaction with IQGAP1, EB1 and microtubules. *J. Cell Sci.* **122**, 2969-2979.
- Yeromin, A. V., Zhang, S. L., Jiang, W., Yu, Y., Safrina, O. and Cahalan, M. D. (2006). Molecular identification of the CRAC channel by altered ion selectivity in a mutant of Orai. *Nature* **443**, 226-229.
- Yu, F., Sun, L. and Machaca, K. (2009). Orai1 internalization and STIM1 clustering inhibition modulate SOCE inactivation during meiosis. *Proc. Natl. Acad. Sci. USA* **106**, 17401-17406.
- Yuan, J. P., Zeng, W., Huang, G. N., Worley, P. F. and Muallem, S. (2007). STIM1 heteromultimerizes TRPC channels to determine their function as store-operated channels. *Nat. Cell Biol.* **9**, 636-645.
- Yuan, J. P., Zeng, W., Dorwart, M. R., Choi, Y. J., Worley, P. F. and Muallem, S. (2009). SOAR and the polybasic STIM1 domains gate and regulate Orai channels. *Nat. Cell Biol.* **11**, 337-343.
- Zeng, W., Yuan, J. P., Kim, M. S., Choi, Y. J., Huang, G. N., Worley, P. F. and Muallem, S. (2008). STIM1 gates TRPC channels, but not Orai1, by electrostatic interaction. *Mol. Cell* **32**, 439-448.
- Zhang, S. L., Yu, Y., Roos, J., Kozak, J. A., Deerinck, T. J., Ellisman, M. H., Stauderman, K. A. and Cahalan, M. D. (2005). STIM1 is a Ca²⁺ sensor that activates CRAC channels and migrates from the Ca²⁺ store to the plasma membrane. *Nature* **437**, 902-905.
- Zhang, S. L., Yeromin, A. V., Zhang, X. H., Yu, Y., Safrina, O., Penna, A., Roos, J., Stauderman, K. A. and Cahalan, M. D. (2006). Genome-wide RNAi screen of Ca²⁺ influx identifies genes that regulate Ca²⁺ release-activated Ca²⁺ channel activity. *Proc. Natl. Acad. Sci. USA* **103**, 9357-9362.
- Zhu-Mauldin, X., Marsh, S. A., Zou, L., Marchase, R. B. and Chatham, J. C. (2012). Modification of STIM1 by O-linked N-acetylglucosamine (O-GlcNAc) attenuates store-operated calcium entry in neonatal cardiomyocytes. *J. Biol. Chem.* **287**, 39094-39106.
- Zumbrunn, J., Kinoshita, K., Hyman, A. A. and Näthke, I. S. (2001). Binding of the adenomatous polyposis coli protein to microtubules increases microtubule stability and is regulated by GSK3 beta phosphorylation. *Curr. Biol.* **11**, 44-49.